Uncertainty quantification analysis of the biological Gompertz model subject to random fluctuations in all its parameters

V. Bevia[a], C. Burgos[a], J.-C. Cortés[a], A. Navarro-Quiles[b,*], R.-J. Villanueva[a]

[a] *Instituto Universitario de Matemática Multidisciplinar, Universitat Politècnica de València, Camino de Vera s/n, 46022, Valencia, Spain*
[b] *Department of Statistics and Operational Research, Universitat de València, Dr Moliner 50, 46100, Burjassot, Spain*

Abstract

In spite of its simple formulation via a nonlinear differential equation, the Gompertz model has been widely applied to describe the dynamics of biological and biophysical parts of complex systems (growth of living organisms, number of bacteria, volume of infected cells, etc.). Its parameters or coefficients and the initial condition represent biological quantities (usually, rates and number of individual/particles, respectively) whose nature is random rather than deterministic. In this paper, we present a complete uncertainty quantification analysis of the randomized Gomperz model via the computation of an explicit expression to the first probability density function of its solution stochastic process taking advantage of the Liouville-Gibbs theorem for dynamical systems. The stochastic analysis is completed by computing other important probabilistic information of the model like the distribution of the time until the solution reaches an arbitrary value of specific interest and the stationary distribution of the solution. Finally, we apply all our theoretical findings to two examples, the first of numerical nature and the second to model the dynamics of weight of a species using real data.

Keywords: Random nonlinear differential equation, Continuity partial differential equation, Liouville-Gibbs theorem, Randomized Gompertz model, Complex systems with uncertainties

1. Introduction

Mathematical models are one of the most powerful formal tools for increasing our understanding about the dynamics of biological and biophysical parts of complex systems [1]. However, deterministic mathematical models are useful to some extent since they neglect random fluctuations and other complex factors that may seriously affect the dynamics of biological systems. For example, in population dynamics studies, these complex factors include weather, genetics, resources, etc. Some important mathematical models, that have been extensively studied

*Corresponding author
Email addresses: vibees@posgrado.upv.es (V. Bevia), clabursi@posgrado.uv.es (C. Burgos), jccortes@imm.upv.es (J.-C. Cortés), ana.navarro@uv.es (A. Navarro-Quiles), rjvillan@imm.upv.es (R.-J. Villanueva)

to describe population dynamics, include the Malthusian, Verhulstian/Logistic and Gompertzian models [2]. Although simple, these models serve as cornerstone to develop more sophisticated mathematical models devised to describe the dynamics of some parts of biological complex systems [3, 4]. Motivated by the foregoing facts, a number of interesting extensions of the above-mentioned deterministic growth population models to the stochastic scenario have been proposed. It is important to point out that these extensions have been done depending on the mathematical properties of the random/stochastic noise introduced in the corresponding deterministic model to formulate its random/stochastic counterpart. Indeed, when the noise is considered via irregular sample paths or trajectories like the Brownian motion or, more generally, the Wiener process, stochastic differential equations (SDEs) are formulated. Whereas random differential equations (RDEs) are those where noise or random fluctuations have regular sample behaviour (continuity, differentiability, bounded variation, etc.) and they are directly manifested by assigning appropriate probability distributions to input data (initial/boundary conditions, forcing/control terms, coefficients). The rigorous handling of SDEs requires special mathematical tools like Itô or Malliavin stochastic calculus [5, 6, 7, 8, 9]. Under this approach noise is prefixed by specific patterns like Gaussian or Lévy stochastic processes. SDEs have found fruitful applications in many scientific areas, particularly in Finance [10, 11]. Complementary, RDEs are rigorously solved using an extension of classical Newton-Leibniz calculus, usually termed mean square calculus. Under this approach, the main mathematical properties of stochastic processes, like continuity, differentiability and integrability, are characterized via the correlation function associated to the corresponding stochastic process provided it does have finite variance, i.e., it is a second-order stochastic process [12, 13, 14, 15]. A main advantage of RDEs is that a wide range of probability distributions can be allocated for input parameters including the Gaussian distribution. This key fact has stimulated the extensive application of RDEs in dealing with real applications where uncertainties play a major role to properly describe the dynamics of the corresponding phenomenon under analysis using a number of techniques including generalized polynomial chaos, collocation methods, random Fröbenius expansions, equivalent linearization, perturbation techniques, etc., [12, 16, 17, 18].

In the context of SDEs, the classical Malthusian, Verhulstian and Gompertzian models have been studied and applied to model a variety of problems like the price of a stock, the asymptotic analysis of equilibrium states for a single species and tumour cell growth, for example (see [11, 19, 20] and references therein, respectively). Whereas in the setting of RDEs both Malthusian and Verhulst models have also been extensively studied, see for instance [21, 22, 23, 24, 25, 26]. However, to best of our knowledge the randomized Gompertz model has not yet been studied in the framework of RDEs.

As in the deterministic setting, the analysis of the aforementioned models formulated via SDEs and RDEs, includes the existence and uniqueness of solution, the continuous dependence of the solution in terms of the initial data, etc., but also the determination of the main statistical properties of the solution stochastic process such as the mean, the variance and higher moments. A more ambitious and desirable goal is the computation of the finite dimensional distributions (usually called the *fidis*) of the solution. In particular, the computation of the first probability density function (1-PDF) is a major goal since from its integration one can straightforwardly determine any one-dimensional moment (in particular, the mean, the variance, the symmetry and the kurtosis), provided they exist, as well as confidence intervals and the probability that the solution lies in an interval of specific interest. In dealing with SDEs, it is known that the 1-PDF satisfies the Fokker-Planck partial differential equation (PDE) [27, Ch. 5]. However, its computation by solving this important PDE in its general form is still a challenge [28] and most of the contributions mainly focus on determining its solution in particular cases using analytical [29] or numerical techniques [30] or to compute the stationary distribution for particular SDEs [31]. In the context of RDEs, the computation of the 1-PDF has been dealt with mainly using a the so-called Random Variable Transformation (RVT) technique. This important result permits to compute the PDF of an absolutely continuous random vector which comes from mapping another absolutely continuous random vector whose PDF is known. This result states as follows

Theorem 1 (Random Variable Transformation technique). *[12, pp. 24–25]*
Let $\mathbf{V}(\omega) = (V_1(\omega), \ldots, V_k(\omega))^\top$ *and* $\mathbf{W}(\omega) = (W_1(\omega), \ldots, W_k(\omega))^\top$ *be two k-dimensional absolutely continuous random vectors defined on a complete probability space* $(\Omega, \mathcal{F}, \mathbb{P})$*. Let* $\mathbf{r} : \mathbb{R}^k \to \mathbb{R}^k$ *be a one-to-one deterministic transformation of* $\mathbf{V}(\omega)$ *into* $\mathbf{W}(\omega)$*, i.e.,* $\mathbf{W}(\omega) = r(\mathbf{V}(\omega))$*,* $\omega \in \Omega$*. Assume that* $\mathbf{r}$ *is a continuous mapping and has continuous partial derivatives with respect to each component* v_i*,* $1 \le i \le k$*. Then, if* $f_{\mathbf{V}}(v_1, \ldots, v_k)$ *denotes the joint probability density function of the vector* $\mathbf{V}(\omega)$*, and* $\mathbf{s} = \mathbf{r}^{-1} = (s_1(w_1, \ldots, w_k), \ldots, s_k(w_1, \ldots, w_k))$ *represents the inverse mapping of* $\mathbf{r} = (r_1(v_1, \ldots, v_k), \ldots, r_k(v_1, \ldots, v_k))$*, the joint probability density function of the random vector* $\mathbf{W}(\omega)$ *is given by*

$$f_{\mathbf{W}}(w_1, \ldots, w_k) = f_{\mathbf{V}}\left(s_1(w_1, \ldots, w_k), \ldots, s_k(w_1, \ldots, w_k)\right) |\mathcal{J}_k|,$$

where $|\mathcal{J}_k|$*, which is assumed to be different from zero, denotes the absolute value of the Jacobian defined by the following determinant*

$$\mathcal{J}_k = \det \begin{bmatrix} \dfrac{\partial s_1(w_1, \ldots, w_k)}{\partial w_1} & \cdots & \dfrac{\partial s_k(w_1, \ldots, w_k)}{\partial w_1} \\ \vdots & \ddots & \vdots \\ \dfrac{\partial s_1(w_1, \ldots, w_k)}{\partial w_k} & \cdots & \dfrac{\partial s_k(w_1, \ldots, w_k)}{\partial y_k} \end{bmatrix}.$$

When a closed-form solution of the RDE is available, the RVT technique is often useful to obtain an exact expression of the 1-PDF of the solution stochastic process [32, 33]. This method has also been successfully applied to determine the 1-PDF of other random equations (see [34, 35] for its application to solve random difference equations, and [36, 37] to deal with random partial differential equations). The RVT method has demonstrated to be very useful to compute approximations of the 1-PDF of the aforementioned type of random equations in combination with other techniques such as Karhunen-Loève expansions [38, 39], Fröbenius expansions [40], differential transform method [41], the homotopy method [42], numerical schemes [43, 44], etc. The main drawback when applying Theorem 1 is finding the appropriate mapping $\mathbf{r}$ as well as its jacobian $\mathcal{J}_k$.

Complementary to the RVT technique, the 1-PDF can also be computed by means of the Liouville-Gibbs theorem for dynamical systems [45, 46, 47]. This result establishes that the 1-PDF satisfies certain PDE, usually termed Liouville-Gibbs equation, that can be regarded as a particular case of the Fokker-Planck PDE for SDEs, but in the setting of RDEs (later on we will comment further details in this regard). In this paper, we will show the key role played by this PDE to determine the 1-PDF of the randomized Gompertz equation avoiding the application of RVT technique and its aforementioned drawbacks. As far as we know, this is the first time that this kind of analysis is carried out for the randomized Gompertz model.

This paper is organized as follows. In Section 2 we summarize and adapt the main results related to the Liouville-Gibbs theorem that will be required to determine a closed-form expression of the 1-PDF of the solution of the randomized Gompertz model. This is done in Subsection

3.1. Section 3 is completed by computing both the distribution of time until certain number of individual/particles reaches a prefixed level (Subsection 3.2) and the stationary distribution of the solution (Subsection 3.3). In Section 4, all the theoretical results established in Section 3 are illustrated via two examples. Conclusions are shown in Section 5.

We finish this section pointing out that throughout this paper the exponential function will be denoted by e or exp, interchangeably.

2. The Liouville-Gibbs partial differential equation

In this section we introduce the main results about the Liouville-Gibbs PDE that will be required throughout this paper to provide a full probabilistic analysis of the randomized Gompertz equation.

Hereinafter, the triplet $(\Omega, \mathcal{F}, \mathbb{P})$ will denote a complete probabilistic space and $(\mathrm{L}_2(\Omega), \|\cdot\|)$ stands for the Hilbert space of second-order real random variables (i.e., having finite variance), $X : \Omega \to \mathbb{R}$, with the inner product $\langle X, Y\rangle = \mathbb{E}[XY]$, $X, Y \in \mathrm{L}_2(\Omega)$, where $\mathbb{E}[\cdot]$ is the expectation operator and the inferred norm is given by $\|X\| = (\mathbb{E}[X^2])^{1/2}$. Second-order real random vectors, $\mathbf{X} : \Omega \to \mathbb{R}^n$, are defined in a natural way in the Hilbert space $(\mathrm{L}_2^n(\Omega), \|\cdot\|_n)$ whose elements are $\mathbf{X} = (X_1, \ldots, X_n)$, with $X_i \in \mathrm{L}_2(\Omega)$, $1 \le i \le n$, and the norm is defined by $\|\mathbf{X}\|_n = \max\{\|X_i\| : 1 \le i \le n\}$. Given $\mathcal{T} \subset \mathbb{R}^+$, a second-order real stochastic process is a family of second-order real random vectors indexed by elements of $\mathcal{T}$, $\mathbf{X}(t) = \{\mathbf{X} : \mathcal{T} \times \Omega \to \mathbb{R}^n : t \in \mathcal{T}, \omega \in \Omega\}$. In practice, $\mathcal{T} = [t_1, t_2]$, $0 \le t_1 < t_2 \le \infty$ (for convenience we interpret the parameter t as time, so we assume it is nonnegative). As usual, in the previous notation the dependence on the parameter ω is hidden for random quantities. The convergence of sequences of random variables/vectors/stochastic functions in the foregoing norms is usually called mean square convergence and the corresponding concepts of mean square continuity, differentiability and integrability of a stochastic process can be defined in terms of $\|\cdot\|$ and $\|\cdot\|_n$, [12, 13, 15].

Let us consider the following initial value problem (IVP)

$$\begin{cases} \frac{\mathrm{d}\mathbf{X}(t)}{\mathrm{d}t} = \mathbf{g}(t, \mathbf{X}(t)), & t > t_0, \\ \mathbf{X}(t_0) = \mathbf{X}_0, \end{cases} \tag{1}$$

where $\mathbf{g} = (g_1, \ldots, g_n) \in C^1([t_0, +\infty) \times \mathrm{L}_2^n(\Omega), \mathbb{R}^n)$ and $\mathbf{X}_0 \in \mathrm{L}_2^n(\Omega)$.

In the context of dynamical systems, the Liouville-Gibbs theorem states that the PDF, $f(t, \mathbf{x})$, of the solution stochastic process, $\mathbf{X}(t)$, of IVP (1) is an invariant of motion, i.e., the integral

$$\mathcal{J}(t) = \int_{D_t} f(t, \mathbf{x})\, \mathrm{d}\mathbf{x} \tag{2}$$

is independent of t for any domain $D_t \subset \mathbb{R}^n$ (defined in terms of t), i.e.,

$$\frac{\mathrm{d}\mathcal{J}(t)}{\mathrm{d}t} = 0. \tag{3}$$

This important result can be derived using the characteristic function and its relationship with the PDF [12, Ch. 6]. Alternatively, let us consider

$$\mathcal{J}(t+h) = \int_{D_{t+h}} f(t+h, \mathbf{y})\, \mathrm{d}\mathbf{y}. \tag{4}$$

Let us denote by

$$\mathbf{x} = (x_1, \ldots, x_n) \in D_t \quad \text{and} \quad \mathbf{y} = (y_1, \ldots, y_n) \in D_{t+h}$$

the coordinates of arbitrary points in the domain of integration of (2) and (4), respectively. On the one hand, using the theorem of change of variables for integrals, expression (4) can be written on the domain D_t as

$$\mathcal{J}(t+h) = \int_{D_t} f(t+h, \mathbf{y}) \frac{\partial \mathbf{y}}{\partial \mathbf{x}} \, \mathrm{d}\mathbf{x}. \tag{5}$$

On the other hand, let us calculate the two factors, $f(t+h, \mathbf{y})$ and the jacobian $\dfrac{\partial \mathbf{y}}{\partial \mathbf{x}}$, appearing in the previous integral. For the former, let us observe using Taylor's expansion of order 2 that

$$\begin{aligned} f(t+h, \mathbf{y}) &= f(t, \mathbf{x}) + h\left(\frac{\partial f}{\partial x_1}\frac{\mathrm{d}x_1}{\mathrm{d}t} + \ldots + \frac{\partial f}{\partial x_n}\frac{\mathrm{d}x_n}{\mathrm{d}t} + \frac{\partial f}{\partial t}\right) + O(h^2) \\ &= f + h\left(\frac{\partial f}{\partial x_1} g_1 + \ldots + \frac{\partial f}{\partial x_n} g_n + \frac{\partial f}{\partial t}\right) + O(h^2), \end{aligned} \tag{6}$$

where in the last step we have used the shorter notation $f = f(t, \mathbf{x})$ and that $\mathbf{x} = (x_1, \ldots, x_n)$ satisfies the differential equation in (1), so $\dfrac{\mathrm{d}x_i}{\mathrm{d}t} = g_i$, $g_i = g_i(t, x_1, \ldots, x_n)$, $1 \le i \le n$. To compute the jacobian, we apply again Taylor's expansion of order 2 for each component,

$$y_i = x_i + h\frac{\mathrm{d}x_i}{\mathrm{d}t} + O(h^2) = x_i + hg_i + O(h^2), \quad 1 \le i \le n.$$

Then the jacobian $\dfrac{\partial \mathbf{y}}{\partial \mathbf{x}}$ in (5) can be calculated as

$$\begin{aligned} \frac{\partial \mathbf{y}}{\partial \mathbf{x}} &= \det \begin{bmatrix} \dfrac{\partial y_1}{\partial x_1} & \cdots & \dfrac{\partial y_n}{\partial x_1} \\ \vdots & \ddots & \vdots \\ \dfrac{\partial y_1}{\partial x_n} & \cdots & \dfrac{\partial y_n}{\partial x_n} \end{bmatrix} \\ &= \det \begin{bmatrix} 1 + h\dfrac{\partial g_1}{\partial x_1} + O(h^2) & \cdots & h\dfrac{\partial g_n}{\partial x_1} + O(h^2) \\ \vdots & \ddots & \vdots \\ h\dfrac{\partial g_1}{\partial x_n} + O(h^2) & \cdots & 1 + h\dfrac{\partial g_n}{\partial x_n} + O(h^2) \end{bmatrix} \\ &= 1 + h\left(\frac{\partial g_1}{\partial x_1} + \cdots + \frac{\partial g_n}{\partial x_n}\right) + O(h^2). \end{aligned}$$

Therefore, using (6) and this last expression for the jacobian one gets

$$\begin{aligned} f(t+h, \mathbf{y})\frac{\partial \mathbf{y}}{\partial \mathbf{x}} &= \left[f + h\left(\frac{\partial f}{\partial x_1} g_1 + \ldots + \frac{\partial f}{\partial x_n} g_n + \frac{\partial f}{\partial t}\right) + O(h^2)\right] \\ &\quad \cdot \left[1 + h\left(\frac{\partial g_1}{\partial x_1} + \cdots + \frac{\partial g_n}{\partial x_n}\right) + O(h^2)\right] \\ &= f + h\left(\frac{\partial f}{\partial x_1} g_1 + \ldots + \frac{\partial f}{\partial x_n} g_n + \frac{\partial f}{\partial t}\right. \\ &\quad \left. + f\frac{\partial g_1}{\partial x_1} + \cdots + f\frac{\partial g_n}{\partial x_n}\right). \end{aligned}$$

Now, we use the rule for the derivative of a product $\frac{\partial(fg_i)}{\partial x_i} = \frac{\partial f}{\partial x_i} g_i + f \frac{\partial g_i}{\partial x_i}$, $1 \le i \le n$. Then the last expression can be written as

$$f(t+h, \mathbf{y}) \frac{\partial \mathbf{y}}{\partial \mathbf{x}} = f(t, \mathbf{x}) + h \left(\frac{\partial f}{\partial t} + \sum_{i=1}^{n} \frac{\partial (f g_i)}{\partial x_i} \right),$$

i.e.,

$$\frac{f(t+h, \mathbf{y}) \frac{\partial \mathbf{y}}{\partial \mathbf{x}} - f(t, \mathbf{x})}{h} = \frac{\partial f}{\partial t} + \sum_{i=1}^{n} \frac{\partial (f g_i)}{\partial x_i}, \tag{7}$$

where, for convenience, we have recovered the notation $f = f(t, \mathbf{x})$. Finally, we subtract (2) from (4), we divide by h and take limits as $h \to 0$, then taking into account (7), one gets

$$0 = \frac{\mathrm{d}\mathcal{J}(t)}{\mathrm{d}t} = \lim_{h \to 0} \frac{\mathcal{J}(t+h) - \mathcal{J}(t)}{h} = \int_{D_t} \frac{f(t+h, \mathbf{y}) \frac{\partial \mathbf{y}}{\partial \mathbf{x}} - f(t, \mathbf{x})}{h} \mathrm{d}\mathbf{x} = \int_{D_t} \left(\frac{\partial f}{\partial t} + \sum_{i=1}^{n} \frac{\partial (f g_i)}{\partial x_i} \right) \mathrm{d}\mathbf{x}.$$

Therefore, if the PDF $f = f(t, \mathbf{x})$ of the solution stochastic process of (1) satisfies the following PDE

$$\frac{\partial f}{\partial t} + \sum_{i=1}^{n} \frac{\partial (f g_i)}{\partial x_i} = 0 \tag{8}$$

then it is an invariant of motion of the dynamical system (1). This PDE is called the Liouville-Gibbs equation and can be regarded as a particular case of the Fokker-Planck equation associated to the Itô-type SDE

$$\begin{cases} \mathrm{d}\mathbf{X}(t) = \mathbf{g}(t, \mathbf{X}(t))\mathrm{d}t + \boldsymbol{\sigma}(t, \mathbf{X}(t))\mathrm{d}\mathbf{W}(t), \quad t > t_0, \\ \mathbf{X}(t_0) = \mathbf{X}_0, \end{cases}$$

where $\boldsymbol{\sigma} = (\sigma_{ij}) \in C^{1,2}([t_0, +\infty) \times \mathrm{L}_2^n(\Omega), \mathbb{R}^{n \times m})$ and $\mathbf{W}(t)$ is an m-dimensional Wiener process, in the case that the diffusion matrix $\boldsymbol{\sigma} = \mathbf{0}$ [27, 47].

For a given initial PDF, $f_0(\mathbf{x})$, the Liouville-Gibbs equation (8) can be expressed as

$$\begin{cases} \frac{\partial f(t, \mathbf{x})}{\partial t} + \nabla \cdot (f(t, \mathbf{x})\mathbf{g}(t, \mathbf{x})) = 0, \quad t > t_0, \quad \mathbf{x} \in \mathbb{R}^n, \\ f(t_0, \mathbf{x}) = f_0(\mathbf{x}), \quad \mathbf{x} \in \mathbb{R}^n, \end{cases} \tag{9}$$

in terms of the divergence operator $\nabla \cdot (\cdot)$ with respect to the spatial components $\mathbf{x}$. In this form this PDE is usually termed the continuity equation [47, 48].

Developing the divergence of the product, we obtain a more practical form of equation (9)

$$\frac{\partial f(t, \mathbf{x})}{\partial t} + \sum_{k=1}^{n} g_k(t, \mathbf{x}) \frac{\partial f(t, \mathbf{x})}{\partial x_k} = -f(t, \mathbf{x}) \, \nabla \cdot \mathbf{g}(t, \mathbf{x}). \tag{10}$$

Using the Lagrange system associated to this PDE

$$\frac{\mathrm{d}t}{1} = -\frac{\mathrm{d}f}{f \, \nabla \cdot \mathbf{g}(t, \mathbf{x})} = \frac{\mathrm{d}x_1}{g_1} = \cdots = \frac{\mathrm{d}x_n}{g_n},$$

and from the first equality on the above chain of identities, one gets the unique local solution of the Liouville-Gibbs equation [12, Ch. 6]

$$f(t,\mathbf{x}) = f_0(\mathbf{h}^{-1}(t,\mathbf{x}))\exp\left\{-\int_{t_0}^{t} \nabla\cdot\mathbf{g}(s,\mathbf{x}=\mathbf{h}(t,\mathbf{x}_0))\,\mathrm{d}s\right\}\Big|_{\mathbf{x}_0=\mathbf{h}^{-1}(t,\mathbf{x})}. \tag{11}$$

Here, function $\mathbf{X}(t) = \mathbf{h}(t,\mathbf{X}_0)$ solves the differential equation (1) and $\mathbf{X}_0 = \mathbf{h}^{-1}(t,\mathbf{X})$ solves for $\mathbf{X}_0$ the equation $\mathbf{X} = \mathbf{h}(t,\mathbf{X}_0)$ for t arbitrary but fixed, so $\mathbf{X} = \mathbf{X}(t)$. Furthermore, we can see why equation (10) is more practical when obtaining the solution of the continuity equation, namely, the factor $\nabla\cdot\mathbf{g}(t,\mathbf{x})$ of the right-hand side of equation (10) appears directly in the integral that explicitly provides the solution via (11).

So far, we have studied the case where randomness just appears in the initial conditions, however in the analysis of complex systems with uncertainties, and in particular in the randomized Gompertz model, its coefficients can be also affected by random fluctuations that may seriously change the solution. Therefore, it is more realistic to treat the case that both initial condition and coefficients (including the forcing/source term) are also stochastic. This motivates that in our subsequent analysis we consider the following random IVP

$$\begin{cases} \frac{\mathrm{d}\mathbf{X}(t)}{\mathrm{d}t} = \mathbf{g}(t,\mathbf{X}(t),\mathbf{A}), & t > t_0, \\ \mathbf{X}(t_0) = \mathbf{X}_0, \end{cases} \tag{12}$$

where $\mathbf{X}_0 \in \mathrm{L}_2^n(\Omega)$ and $\mathbf{A} \in \mathrm{L}_2^m(\Omega)$. At this point, it is important to point out that we restrict ourselves to the case that the IVP (12) has a finite degree of randomness [12, Ch. 3] via a finite number of second-order random variables $\mathbf{A} = (A_1,\ldots,A_m)$. Although $\mathbf{A}$ is independent of t, we want to stress that our scenario also comprises the case that uncertainties can be considered through many stochastic processes such as polynomials, trigonometric or exponential functions, etc., depending on $A_1,\ldots,A_m$ and t separately. In the case that randomness is defined via stochastic processes having a different nature, like for instance Brownian motion (or its transformations, Brownian bridge, Brownian with drift, etc.), we can still take advantage of our approach by considering its truncated Karhunen-Loève expansions [49]. Therefore, our setting can be applied in a wide range of practical cases.

Considering the conditional PDF of the solution stochastic process with respect to the values of $\mathbf{A}$, $f(t,\mathbf{x}|\mathbf{a})$, we know that it verifies the continuity equation (9)

$$\frac{\partial f(t,\mathbf{x}|\mathbf{a})}{\partial t} + \nabla\cdot(f(t,\mathbf{x}|\mathbf{a})\mathbf{g}(t,\mathbf{x};\mathbf{a})) = 0. \tag{13}$$

Observe that this holds because when we consider the conditional density, we are actually assuming an arbitrary, but fixed, value for $\mathbf{A} = \mathbf{a}$. Therefore, although $\mathbf{a}$ is written as an entry of function $\mathbf{g}$, it does not play the role of a variable but a fixed parameter, so it verifies the continuity equation. Let $f_{\mathbf{A}}$ denote the joint PDF of the random variables appearing in the differential equation. Then, we can multiply both sides of (13) by this density and, therefore

$$\frac{\partial (f(t,\mathbf{x}|\mathbf{a})f_{\mathbf{A}}(\mathbf{a}))}{\partial t} + \nabla\cdot(f(t,\mathbf{x}|\mathbf{a})f_{\mathbf{A}}(\mathbf{a})\mathbf{g}(t,\mathbf{x};\mathbf{a})) = 0,$$

i.e.,

$$\frac{\partial f(t,\mathbf{x},\mathbf{a})}{\partial t} + \nabla\cdot(f(t,\mathbf{x},\mathbf{a})\mathbf{g}(t,\mathbf{x};\mathbf{a})) = 0, \tag{14}$$

where we have used the following relationship between the conditional PDF, $f(t, \mathbf{x}|\mathbf{a})$, the joint PDF, $f(t, \mathbf{x}, \mathbf{a})$ and the marginal, $f_{\mathbf{A}}(\mathbf{a})$, namely $f(t, \mathbf{x}|\mathbf{a}) f_{\mathbf{A}}(\mathbf{a}) = f(t, \mathbf{x}, \mathbf{a})$. Similarly to the case where randomness is only in the initial condition, it can be seen that the solution of (14) together with the initial condition $f_0(\mathbf{x}_0, \mathbf{a})$ is given by

$$f(t, \mathbf{x}, \mathbf{a}) = f_0(\mathbf{h}^{-1}(t, \mathbf{x}, \mathbf{a}), \mathbf{a}) \exp\left\{ - \int_{t_0}^{t} \nabla \cdot \mathbf{g}(s, \mathbf{x} = \mathbf{h}(s, \mathbf{x}_0, \mathbf{a}); \mathbf{a}) \, \mathrm{d}s \right\} \Big|_{\mathbf{x}_0 = \mathbf{h}^{-1}(t, \mathbf{x}, \mathbf{a})}, \qquad (15)$$

where we first solve (12) obtaining $\mathbf{X}(t) = \mathbf{h}(t, \mathbf{X}_0, \mathbf{A})$ and then $\mathbf{X}_0$ solves the equation $\mathbf{X}_0 = \mathbf{h}^{-1}(t, \mathbf{X}, \mathbf{A})$ for t fixed. Now, to determine the 1-PDF of the solution stochastic process, we have to integrate with respect to the random coefficients $\mathbf{A} = (A_1, \ldots, A_m)$, obtaining

$$f(t, \mathbf{x}) = \int_{\mathbb{R}^m} f(t, \mathbf{x}, \mathbf{a}) \, \mathrm{d}\mathbf{a}. \qquad (16)$$

3. The randomized Gompertz model

This section is addressed to determine the main probabilistic properties of the randomized Gompertz model, namely, the 1-PDF of its solution stochastic process, the distribution of the time until a certain number of the individuals (also termed particles, depending upon the context of the problem) reaches a prefixed level and, finally, the stationary distribution. All this crucial information is presented in the following subsections. The main mathematical tools that will be applied to conduct our subsequent study are the Liouville-Gibbs PDE and the so called RVT technique. The former is required to determine the 1-PDF of the randomized Gompertz model and the latter to compute both the distribution of the time and the stationary distribution.

3.1. Computing the 1-PDF of the randomized Gompertz model

The aim of this subsection is to obtain an explicit expression for the 1-PDF, $f(t, n)$, of the following Gompertz model

$$\begin{cases} N'(t) = N(t)[C - B \ln(N(t))], & t > t_0 \geq 0, \\ N(t_0) = N_0, \end{cases} \qquad (17)$$

where N_0, B and C are second-order random variables and the unknown $N(t)$ is a second-order stochastic process. Here $N(t)$ can represent the number of cells/organisms, weight or other biological magnitudes, being N_0 its initial value at the time instant t_0. Parameters $B > 0$ and $C > 0$ represent the growth rate (division rate in the case of cells) of the system and difference between the growth and "dampening factor" rates (death rate in the case of cells), respectively [50]. Observe that according to the development exhibited in Section 2, comparing (17) with the general problem (12) and its notation, now $n = 1$ ($\mathbf{X}(t) \equiv X(t) = N(t)$), $m = 2$ ($\mathbf{A} = (B, C)$) and $\mathbf{g}(t, \mathbf{X}(t), \mathbf{A}) = g(t, N(t), B, C) = g_1(t, N(t), B, C) = N(t)\,[C - B \ln(N(t))]$. Using the notation $n = n(t)$, the Liouville-Gibbs equation (14) writes

$$\begin{cases} \dfrac{\partial f(t, n, b, c)}{\partial t} + \nabla \cdot (f(t, n, b, c)\, n(c - b \ln(n))) = 0, & t > t_0, \quad n > 0, \\ f(t_0, n, b, c) = f_0(n_0, b, c), \end{cases}$$

where f_0 is the joint density of the random variables N_0, B and C.

To obtain the solution by expression (16), we first need to calculate (15). To this end, we must obtain the divergence term and function $n(t) = h(t, n_0, b, c)$. On the one hand, $g(t, n) = n(c - b\ln(n))$, so its divergence with respect to the "spatial" components is its derivative with respect to n, i.e.,

$$\nabla \cdot g(t, n) = c - b(\ln(n) + 1).$$

On the other hand, it is well-known that the solution of the Gompertz model (17) is given by

$$n = h(t, n_0, b, c), \quad \text{where} \quad h(t, n_0, b, c) = \mathrm{e}^{-\frac{c\left(\mathrm{e}^{-b(t-t_0)}-1\right)}{b}} n_0^{\mathrm{e}^{-b(t-t_0)}}. \tag{18}$$

Therefore, solving for n_0 gives

$$n_0 = h^{-1}(t, n, b, c) = n^{\mathrm{e}^{b(t-t_0)}} \mathrm{e}^{-\frac{c}{b}(\mathrm{e}^{b(t-t_0)}-1)}. \tag{19}$$

Applying expression (15), we obtain

$$\begin{aligned} f(t, n, b, c) &= f_0(h^{-1}(t, n, b, c), b, c) \exp\left\{-\int_{t_0}^{t} c - b(\ln(h(s, n_0, b, c)) + 1)\,\mathrm{d}s\right\}\Big|_{n_0=h^{-1}(t,n,b,c)} \\ &= f_0(h^{-1}(t, n, b, c), b, c) \exp\left(\eta(t, n, b, c)\right), \end{aligned} \tag{20}$$

where, after calculating the integral and performing its evaluation at $n_0 = h^{-1}(t, n, b, c)$ given by (19) one gets

$$\begin{aligned} \eta(t, n, b, c) &= b(t - t_0) + \tfrac{c}{b}\left(\mathrm{e}^{b(t-t_0)} - 1\right) + ct\mathrm{e}^{b(t-t_0)} \\ &\quad -\left(\mathrm{e}^{b(-t+t_0)}(1 + bt) - 1\right)\ln\left[\mathrm{e}^{-\frac{c\left(-1+\mathrm{e}^{b(t-t_0)}\right)}{b}} n^{\mathrm{e}^{b(t-t_0)}}\right] \\ &\quad +bt\ln\left[\mathrm{e}^{-\frac{c\left(-1+\mathrm{e}^{b(-t+t_0)}\right)}{b}}\left(\mathrm{e}^{-\frac{c\left(-1+\mathrm{e}^{b(t-t_0)}\right)}{b}} n^{\mathrm{e}^{b(t-t_0)}}\right)^{\mathrm{e}^{b(-t+t_0)}}\right]. \end{aligned} \tag{21}$$

Finally, we apply expression (16) to determine the PDF of the solution stochastic process of the randomized Gompertz model (17) by marginalizing

$$f(t, n) = \int_{\mathbb{R}^2} f(t, n, b, c)\,\mathrm{d}b\,\mathrm{d}c, \tag{22}$$

where $f(t, n, b, c)$ is given by (19)–(21). In the case that the N_0, B and C are independent random variables, then $f_0(n_0, b, c) = f_{N_0}(n_0) f_B(b) f_C(c)$ and (20) writes

$$f(t, n, b, c) = f_{N_0}(h^{-1}(t, n, b, c)) f_B(b) f_C(c) \exp\left(\eta(t, n, b, c)\right). \tag{23}$$

Finally, observe that once the 1-PDF $f(t, n)$ has been determined, the computation of the one-dimensional moments turn easily out provided they exist. For instance, the mean and the standard deviation are given by

$$\mu_N(t) = \mathbb{E}[N(t)] = \int_{\mathbb{R}} n f(t, n)\,\mathrm{d}n, \tag{24}$$

and

$$\sigma_N(t) = \sqrt{\int_{\mathbb{R}} n^2 f(t, n, b, c)\,\mathrm{d}n - (\mu_N(t))^2}, \tag{25}$$

respectively.

3.2. The distribution of the time until a certain number of individuals reaches a prefixed level

The Gompertz model describes the dynamics of $N(t)$ over the time t. In this setting a crucial question that often arises in research is to determine when $N(t)$ reaches a specific value of interest, say ρ_N. In other words, we may be interested in determining the time instant $T_{\rho_N} := T$ such that $N(t) = \rho_N$. In our context, $N(t) = N(t; N_0, B, C)$ depends on model parameters N_0, B and C, which are random variables, so the time T is also a random variable. Hereinafter, we derive the distribution of T under very general hypotheses on N_0, B and C taking advantage of the RVT method stated in Theorem 1.

To this end, let us fix a value $\rho_N > 0$. Then, the solution (18) can be expressed as (observe that for convenience the model parameters and time are written using capital letters since now they are interpreted as random variables)

$$\rho_N = \mathrm{e}^{-\frac{C\left(\mathrm{e}^{-B(T-t_0)}-1\right)}{B}} N_0^{\mathrm{e}^{-B(T-t_0)}}.$$

According to Theorem 1 with $k = 3$, let us consider the following identification $\mathbf{V} = (V_1, V_2, V_3) = (N_0, B, C)$ and $\mathbf{W} = (W_1, W_2, W_3)$ with the following transformation $\mathbf{r} : \mathbb{R}^3 \longrightarrow \mathbb{R}^3$ whose components $r_i(\mathbf{v})$, $i = 1, 2, 3$, are given by

$$\begin{aligned} w_1 &= r_1(\mathbf{v}) = t = t_0 - \frac{1}{b} \ln\left(\frac{\ln(\rho_N) - \frac{c}{b}}{\ln(n_0) - \frac{c}{b}}\right), \\ w_2 &= r_2(\mathbf{v}) = b, \\ w_3 &= r_3(\mathbf{v}) = c. \end{aligned}$$

Now, we compute the inverse mapping of $\mathbf{r}$: $\mathbf{s}(\mathbf{w}) = \mathbf{r}^{-1}(\mathbf{v})$, whose components s_i, $1 \le i \le 3$, are

$$\begin{aligned} n_0 &= s_1(\mathbf{w}) = \rho_N^{\mathrm{e}^{w_2(w_1-t_0)}} \mathrm{e}^{-\frac{w_3}{w_2}(\mathrm{e}^{w_2(w_1-t_0)}-1)}, \\ b &= s_2(\mathbf{w}) = w_2, \\ c &= s_3(\mathbf{w}) = w_3. \end{aligned}$$

The absolute value of the jacobian of this transformation $\mathbf{s}$ is

$$|J| = \left|\det\begin{bmatrix} \frac{\partial n_0}{\partial w_1} & 0 & 0 \\ \frac{\partial n_0}{\partial w_2} & 1 & 0 \\ \frac{\partial n_0}{\partial w_3} & 0 & 1 \end{bmatrix}\right| = \left|\frac{\partial n_0}{\partial t}(w_1, w_2, w_3)\right| = \rho_N^{\mathrm{e}^{w_2(w_1-t_0)}} \mathrm{e}^{-\frac{w_3}{w_2}(\mathrm{e}^{w_2(w_1-t_0)}-1)} |w_2 \ln(\rho_N) - w_3| \mathrm{e}^{w_2(w_1-t_0)}.$$

Therefore, applying Theorem 1 the distribution of time T for a given value ρ_N of N is given by

$$f_T(t, \rho_N) = \int_{\mathbb{R}^2} f_0(\rho_N^{\mathrm{e}^{b(t-t_0)}} \mathrm{e}^{-\frac{c}{b}(\mathrm{e}^{b(t-t_0)}-1)}, b, c) \rho_N^{\mathrm{e}^{b(t-t_0)}} \mathrm{e}^{-\frac{c}{b}(\mathrm{e}^{b(t-t_0)}-1)} |b \ln \rho_N - c| \mathrm{e}^{b(t-t_0)} \,\mathrm{d}b\,\mathrm{d}c, \tag{26}$$

where $f_0(n_0, b, c)$ denotes the joint PDF of the random vector (N_0, B, C). If we assume independence between the model parameters N_0, B and C, f_0 would factorize as the product of the corresponding marginals f_{N_0}, f_B and f_C.

An important information that will be utilized later in the Example 2 is the average time of random variable $T := T_{\rho_N}$ for a fixed value of ρ_N. This quantity is now straightforwardly obtained once the PDF of T has been determined,

$$\mu_T(\rho_N) := \mathbb{E}[T_{\rho_N}] = \mathbb{E}[T] = \int_{\mathbb{R}} t f_T(t, \rho_N)\,\mathrm{d}t = \int_{t_0}^{+\infty} t f_T(t, \rho_N)\,\mathrm{d}t, \tag{27}$$

where $f_T(t, \rho_N)$ is given by (26).

3.3. Stationary distribution of the solution

In this section, we will take advantage of the RVT technique to calculate the probability distribution of the stationary state. Taking limits as $t \to \infty$ in expression (18) it is straightforward to check that the steady-state of the randomized Gompertz model is the random variable $N^* = \mathrm{e}^{C/B}$. To compute its PDF we will apply Theorem 1 with $k = 2$, $\mathbf{V} = (V_1, V_2) = (B, C)$, $\mathbf{W} = (W_1, W_2)$ and the following deterministic mapping, $\mathbf{r} : \mathbb{R}^2 \to \mathbb{R}^2$, $\mathbf{r}(\mathbf{v}) = (r_1(\mathbf{v}), r_2(\mathbf{v}))$ where

$$w_1 = r_1(\mathbf{v}) = \mathrm{e}^{c/b}, \qquad w_2 = r_2(\mathbf{v}) = b.$$

Then, its inverse mapping, $\mathbf{s} : \mathbb{R}^2 \to \mathbb{R}^2$, is

$$b = s_1(\mathbf{w}) = w_2, \qquad c = s_2(\mathbf{w}) = w_2 \ln(w_1).$$

The absolute value of the Jacobian of mapping $\mathbf{s}$ can be easily calculated

$$|J_2| = \left| \det \begin{bmatrix} 0 & \frac{w_2}{w_1} \\ 1 & \ln(w_1) \end{bmatrix} \right| = \left| -\frac{w_2}{w_1} \right| = \frac{w_2}{w_1}.$$

The last equality holds since both $\mathbb{P}\left[\{\omega \in \Omega : \mathrm{e}^{c(\omega)/b(\omega)} > 0\}\right] = 1$ and $\mathbb{P}\left[\{\omega \in \Omega : b(\omega) > 0\}\right] = 1$. Therefore, the PDF of the random vector (N^*, B) is

$$f_{N^*,B}(w_1, w_2) = f_{B,C}\left(w_2, w_2 \ln(w_1)\right) \frac{w_2}{w_1}. \tag{28}$$

Since we are assuming that the PDF f_0 of model parameters, (N_0, B, C), is known, then the PDF of random vector (B, C) is given by

$$f_{B,C}(b, c) = \int_{\mathbb{R}} f_0(n_0, b, c)\, \mathrm{d}n_0.$$

So, applying this in (28) and taking into account that $w_1 = n^*$ and $w_2 = b$, one obtains

$$f_{N^*,B}(n^*, b) = \frac{b}{n^*} \int_{\mathbb{R}} f_0(n_0, b, b \ln(n^*))\, \mathrm{d}n_0.$$

Finally, we can determine the PDF of the stationary state marginalizing this distribution with respect to random variable B. This yields

$$f_{N^*}(n^*) = \frac{1}{n^*} \int_{\mathbb{R}} \int_{\mathbb{R}} b\, f_0(n_0, b, b \ln(n^*))\, \mathrm{d}n_0\, \mathrm{d}b. \tag{29}$$

In the usual case where all input parameters are independent random variables, the previous expression can be simplified as

$$f_{N^*}(n^*) = \frac{1}{n^*} \int_{\mathbb{R}} b f_B(b)\, f_C(b \ln(n^*))\, \mathrm{d}b, \tag{30}$$

since $f_0(n_0, b, b\ln(n)) = f_{N_0}(n_0) f_B(b) f_C(b \ln(n))$ (where f_{N_0}, f_B and f_C denote the PDFs of random variables N_0, B and C, respectively) and $\int_{\mathbb{R}} f_{N_0}(n_0)\, \mathrm{d}n_0 = 1$.

Remark 1. Observe that since C is a positive random variable, in practice the domain of integration in (30) must be calculated taking into account that the term $b \ln(n^*)$ must be positive. Even more, since B is also a positive random variable, then $N^*(\omega) > 1$ for all $\omega \in \Omega$. This fact will be used later in Example 2.

4. Examples

In this section we present two examples. Example 1 is devised to illustrate the application of the theoretical results established throughout Section 3 considering statistical dependence/independence of model parameters N_0, B and C. The nature in this example is just numerical. We complete this section including a second example where we show how to describe the dynamics of a biological process using real data via Gompertz model. In both examples we calculate the 1-PDF of the solution stochastic process, its mean and standard deviation functions together with confidence intervals as well as the stationary distribution. Additionally, we compute the PDF the random variable time T as defined in Section 3.2.

Example 1. *In this numerical example we will examine two scenarios with respect to dependence/independence of model parameters N_0, B and C and its impact on the Gompertz model output. To this end, we will first consider that the random vector (N_0, B, C) has a Multinormal distribution whose variance-covariance matrix, say Σ, is non-diagonal (so, N_0, B and C are dependent random variables) and, secondly, when Σ is diagonal (so, N_0, B and C are independent random variables). Then we show how the 1-PDF of the solution stochastic process, the mean and standard deviation functions, the PDF of the time random variable and the stationary distribution change in each scenario.*

- *Scenario 1 (dependence): The random vector (N_0, B, C) has a Multinormal distribution truncated to $\mathcal{T} = \mathbb{R}^+ \times \mathbb{R}^+ \times \mathbb{R}^+$, $(N_0, B, C) \sim \mathrm{N}_{\mathcal{T}}(\boldsymbol{\mu}, \boldsymbol{\Sigma})$, with the following mean vector and variance-covariance matrix*

$$\boldsymbol{\mu} = (0.8, 1, 1.5), \quad \boldsymbol{\Sigma} = \frac{1}{10}\begin{bmatrix} 1 & 0 & 1 \\ 0 & 1.2 & 1 \\ 1 & 1 & 2 \end{bmatrix}, \tag{31}$$

respectively. Then, the PDF of random vector (N_0, B, C) is

$$f_0(n_0, b, c) = \begin{cases} 0.001676\, \mathrm{e}^{-25b^2 - 30c^2 + b(15+50c-50n_0) + (16-35n_0)n_0 + c(-8+60n_0)}, & n_0, b, c > 0, \\ 0, & \textit{in other case}. \end{cases} \tag{32}$$

- *Scenario 2 (independence): The random vector (N_0, B, C) has a Multinormal distribution truncated to $\mathcal{T} = \mathbb{R}^+ \times \mathbb{R}^+ \times \mathbb{R}^+$, $(N_0, B, C) \sim \mathrm{N}_{\mathcal{T}}(\mu, \Sigma)$, with the following mean vector and variance-covariance matrix*

$$\boldsymbol{\mu} = (0.8, 1, 1.5), \quad \boldsymbol{\Sigma} = \frac{1}{10}\begin{bmatrix} 1 & 0 & 0 \\ 0 & 1.2 & 0 \\ 0 & 0 & 2 \end{bmatrix}, \tag{33}$$

respectively. Then, the PDF of random vector (N_0, B, C) is

$$f_0(n_0, b, c) = f_{N_0}(n_0) f_B(b) f_C(c) = \begin{cases} 1.30656\, \mathrm{e}^{-4.17(-1+b)^2 - 2.5(-1.5+c)^2 - 5(-0.8+n_0)^2} & n_0, b, c > 0, \\ 0 & \textit{in other case}. \end{cases} \tag{34}$$

In Figure 1 we show the 1-PDF, $f(t, n)$, of the solution stochastic process for different time instants in the interval $[0, 1]$ in both scenarios. To compute $f(t, n)$ in the scenario 1, we have *used expressions* (22) *together with* (19)–(21) *where* f_0 *is given by* (32)*. While to compute* $f(t, n)$ *in the scenario 2, we have applied* (22)*,* (19)*,* (21) *and* (23) *where* f_0 *is given by* (34)*. From this graphical representation we can observe that the 1-PDF corresponding to scenario 2 is more leptokurtic than in the scenario 1. This fact is in agreement with the results shown in Figure 2 where the expectation (calculated via* (24)*) and the standard deviation (calculated via* (25)*) in each scenario are compared. In Figure 2 we see that the variability of the solution is, in general, greater considering dependent random inputs (scenario 1). We observe that near the time instant* $t = 1$*, the variability in the dependent case is smaller than in the independent one. This fact can be explained from Figure 3 since at* $t = 1$ *we see that the right-tail of the PDF,* $f(n, 1)$*, obtained in the scenario 2 is heavier than in scenario 1.*

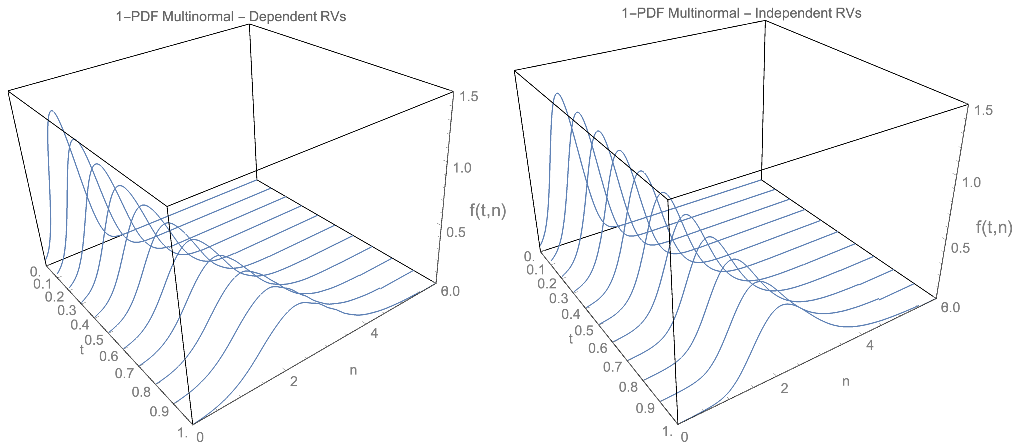

Figure 1: 1-PDF of the solution stochastic process, $f(t, n)$, of the Gompertz model (17) whose input is a multinormal distribution $(N_0, B, C) \sim \mathrm{N}_{\mathcal{T}}(\boldsymbol{\mu}, \boldsymbol{\Sigma})$, at different time instants in the interval $[0, 1]$, in both scenarios. Left (scenario 1-dependent random variables (RVs)): $\boldsymbol{\mu}$ and $\boldsymbol{\Sigma}$ are given by (31). Right (scenario 2-independent RVs): $\boldsymbol{\mu}$ and $\boldsymbol{\Sigma}$ are given by (33). Example 1.

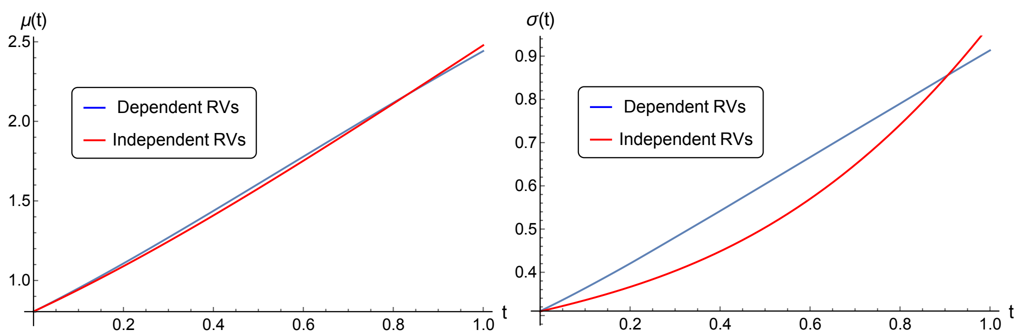

Figure 2: Expectation (left), $\mu(t)$, and standard deviation (right), $\sigma(t)$, in scenario 1 (dependent random variables (RVs)) and in scenario 2 (independent RVs) in the time interval $[0, 1]$. Example 1.

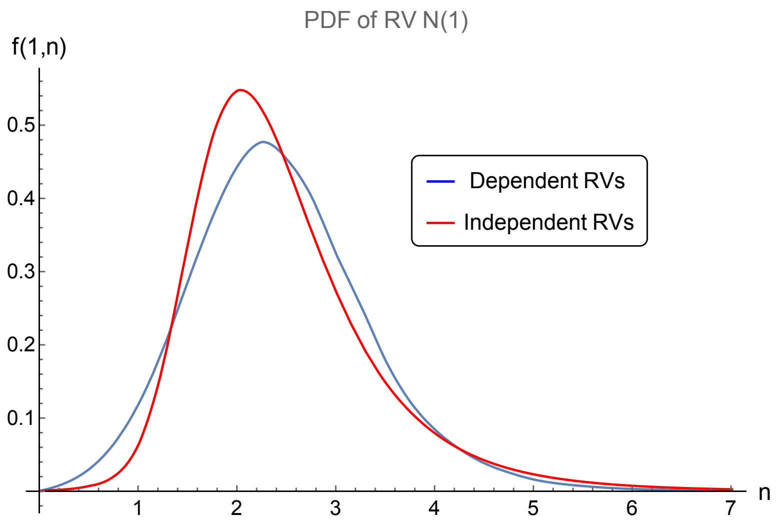

Figure 3: PDF of the solution stochastic process in the time instant $t = 1$, $f(1, n)$, in scenario 1 (dependent random variables (RVs)) and in scenario 2 (independent RVs). Example 1.

According to Subsection 3.2 we can also compute the PDF of the time T until a certain number of individuals/particles reach a fixed value, ρ_N. In Figure 4 we show the PDF of T for different values of $\rho_N \in \{1, 1.25, 1.5, 1.75, 2, 2.25, 2.50\}$. By applying (27)*, in Table 1 we collect the expectation of T for the different values of ρ_N in scenarios 1 and 2. To carry out computations, we have used expressions* (27) *and* (26)*, taking f_0 the PDF defined in* (32) *(in scenario 1) and* (34) *(in scenario 2). With data chosen in our numerical experiments, we observe that in the case of independent random inputs (scenario 2), the time $\mu_T(\rho_N)$ needed to reach each prefixed value ρ_N is smaller than in the dependent case (scenario 1).*

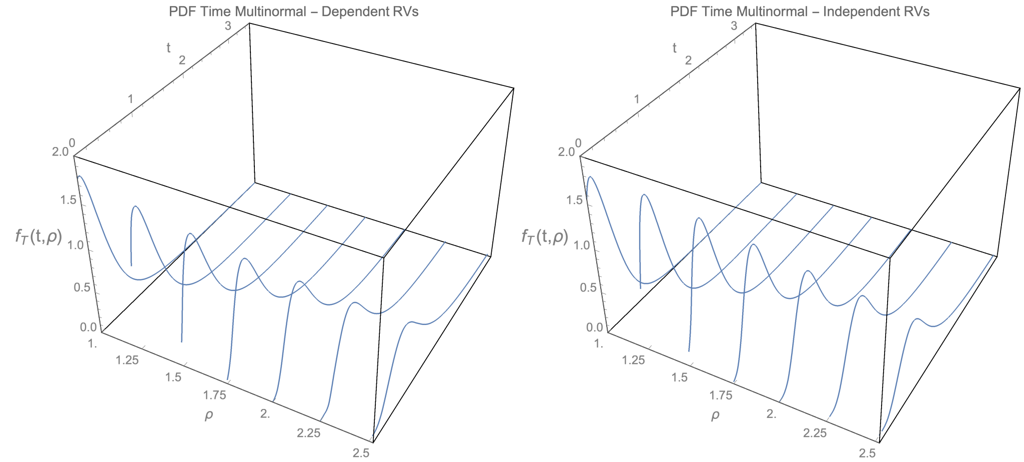

Figure 4: PDF of the time T until a given number of individuals reach a fixed value $\rho = \rho_N \in \{1, 1.25, 1.5, 1.75, 2, 2.25, 2.50\}$. Left (scenario 1-dependent random variables (RVs)). Right (scenario 2-independent RVs). Example 1.

ρ_N	1	1.25	1.5	1.75	2	2.25	2.5
$\mu_T(\rho_N)$ Dep.	0.23233	0.414261	0.592096	0.774202	0.967645	1.17377	1.38623
$\mu_T(\rho_N)$ Indep.	0.169975	0.359007	0.551017	0.745765	0.934527	1.10648	1.25512

Table 1: Expectation of the time needed to reach certain fixed values, $\rho_N \in \{1, 1.25, 1.5, 1.75, 2, 2.25, 2.50\}$ in the scenario 1 (dependent random variables) and in scenario 2 (independent random variables). Example 1.

Finally, we compute the distribution of the stationary state $N^* = \mathrm{e}^{C/B}$*, using the results derived in Subsection 3.3. In Figure 5 we have plotted the PDF of* N^**,* $f_{N^*}(n^*)$ *from expressions* (29) *(scenario 1) and* (30) *(scenario 2). In this latter case, observe that* f_B *and* f_C *correspond to the PDF of the following Gaussian random variables* $B \sim \mathrm{N}(\mu_B = 1; \sigma_B^2 = 12/100)$ *and* $C \sim \mathrm{N}(\mu_C = 15/10; \sigma_C^2 = 2/10)$*. From Figure 5 we observe, that in this particular case, the stationary corresponding to scenario 2 has a heavier right-tail.*

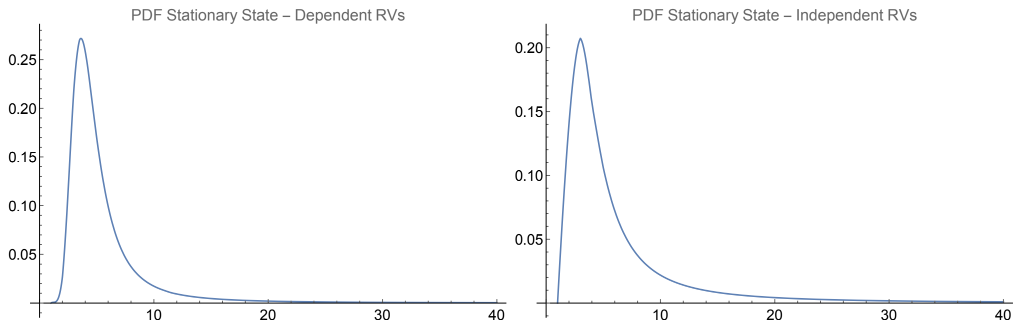

Figure 5: PDFs of the stationary state for each scenario. Left: scenario 1-dependent random variables (RVs). Right: scenario 2-independent RVs. Example 1.

Example 2. *In real applications, the Gompertz model is used to explain the dynamics of data that has been sampled. This model has been used to explain the growth of species, tumors, etc., via measurements like weight, volume, etc. In this example, we use data corresponding to weight measurements, in kilograms, for a randomly bred male Pearl Gray Guinea Fowl population during 23 consecutive days [51]. We have assumed that model parameters are independent random variables and, for them, we choose the following distributions:*

$N_0 \sim \mathrm{U}([0.019779, 0.032472])$ (*uniform distribution*),
$B \sim \mathrm{G}(3841.397958, 0.000057)$ (*gamma distribution*),
$C \sim \mathrm{N}|_{\mathcal{T}}(0.105982, 0.002643)$ (*normal distribution truncated in the interval* $\mathcal{T} = (0.09, 0.12)$).

Now, we justify the selection made for the above-mentioned distributions of each model input. We will assume independence between N_0, B and C since, from a computational point of view, this assumption simplifies the calculations. Anyway, the subsequent computations may be carried out in the case that input parameters are statistically dependent as was shown in Example 1. For the sake of clarity, down below, we explain, in several steps, the underlying reasoning to select the probability distribution of each model input as well as how we have calculated their corresponding parameters.

Step 1: *Initially, the model inputs whose information is more limited are B and C. We only know that both are positive. So, we are going to assign them positive distributions having certain flexibility (specifically, having two degree of freedom, i.e., two parameters, and whose respective shape's density probability varies with such parameters) so that we can better capture their intrinsic uncertainty. Specifically, we will assume that B has a Gamma distribution with parameters $b_1, b_2 > 0$, $B \sim \mathrm{G}(b_1, b_2)$, and C has a Normal distribution with mean, $\mu > 0$, and standard deviation, $\sigma > 0$, truncated in certain interval $\mathcal{T} \subset \mathbb{R}^+$, $\mathrm{N}|_{\mathcal{T}}(\mu, \sigma)$. For the initial condition N_0 we will assume that it has a Uniform distribution in the interval $[n_{0,1}, n_{0,2}]$. These six parameters (b_1, b_2), (μ, σ) and $(n_{0,1}, n_{0,2})$ together with the interval $\mathcal{T}$ will be determined later.*

Step 2: *We first calculate (deterministic) values for model inputs n_0, b and c that best fit, in the mean square sense, the sampled data. We have used the command "NonlinearModelFit"* *(by Mathematica© software) that provides the estimates of model inputs and their errors,*

$$\begin{array}{rclrcl} n_0 &=& 0.026615, & \epsilon_{n_0} &=& 0.000776,\\ b &=& 0.226409, & \epsilon_b &=& 0.003654,\\ c &=& 0.1046, & \epsilon_c &=& 0.002296. \end{array}$$

These (deterministic) estimates will be used later to determine the parameters, $(n_{0,1}, n_{0,2})$, (b_1, b_2) *and* (μ, σ), *of the probability distributions, assigned in Step 1, to each model input* N_0, *B and C, respectively. Specifically, we will consider that the previous values for* (n_0, ϵ_{n_0}), (b, ϵ_b) *and* (c, ϵ_c) *represent (approximately) their means and standard deviations, respectively. As, initially, we are assuming that C has a Normal distribution with mean* $c = 0.1046$ *and standard deviation* $\epsilon_c = 0.002296$, *truncated a certain interval* $\mathcal{T}$ *to be determined, we take* $\mathcal{T}$ *large enough so that it contains its total probability density. We will take, for example,* $\mathcal{T} = (0.09, 0.12)$ *since* $\mathbb{P}[\{\omega \in \Omega : 0.09 < C(\omega) < 0.12\}] \approx 1$, *i.e.*

$$\int_{0.09}^{0.12} \frac{1}{\sqrt{2\,\pi\, 0.002296^2}}\, \mathrm{e}^{-\frac{1}{2}\left(\frac{c-0.1046}{0.002296}\right)^2}\, \mathrm{d}c \approx 1.$$

Step 3: Now, we will determine the parameters $(n_{0,1}, n_{0,2})$, (b_1, b_2) *and* (μ, σ) *by minimizing the mean square error between sampled data,* n_j, $0 \le j \le 22$, *and the expectation of the solution stochastic process* $N(t) = N(t; n_{0,1}, n_{0,2}, b_1, b_2, \mu, \sigma)$ *evaluated at the time instants* $t = t_j$, $0 \le j \le 22$:

$$\min_{n_{0,1}, n_{0,2}, b_1, b_2, \mu, \sigma > 0} \mathrm{E}(n_{0,1}, n_{0,2}, b_1, b_2, \mu, \sigma) = \sum_{j=0}^{22} \left(\mathbb{E}\left[N(t_j; n_{0,1}, n_{0,2}, b_1, b_2, \mu, \sigma) \right] - n_j \right)^2, \tag{35}$$

where the above expectation is computed using expression (24). *In order to calculate the minimum of the above error function* E, *we have used the Nelder-Mead algorithm. Nelder-Mead is a simplex-type method that requires an initial value (seed) to apply it. We use the deterministic information shown in Step 2 to set the starting values that, hereinafter, will be denoted by* $(n_{0,1}^0, n_{0,2}^0)$, (b_1^0, b_2^0) *and* (μ^0, σ^0). *The starting values for random variable C match, obviously, the mean and standard deviation calculated via the deterministic fitting shown in Step 2, so* $\mu^0 = 0.1046$ *and* $\sigma^0 = 0.002296$. *For* N_0, *we calculate* $(n_{0,1}^0, n_{0,2}^0)$ *using the Moment Matching Method [52] for the mean and the variance of a Uniform distribution,*

$$0.026615 = \mathbb{E}[N_0] = \frac{n_{0,1}^0 + n_{0,2}^0}{2}, \qquad 0.000776^2 = \mathbb{V}[N_0] = \frac{(n_{0,2}^0 - n_{0,1}^0)^2}{12}.$$

Solving the above nonlinear system, we obtain $n_{0,1}^0 = 0.020285$ *and* $n_{0,2}^0 = 0.032944$. *Similarly, we calculate the estimates* $b_1^0 = 3838.25$ *and* $b_2^0 = 0.000059$ *solving the system*

$$0.226409 = \mathbb{E}[B] = b_1^0 b_2^0, \qquad 0.003654^2 = \mathbb{V}[B] = b_1^0 \left(b_2^0\right)^2.$$

With this starting value, the error is $\mathrm{E}(n_{0,1}^0, n_{0,2}^0, b_1^0, b_2^0, \mu^0, \sigma^0) = 0.011507$. *After minimizing the objective function* (35), *we obtain*

$$\begin{array}{rclrclrcl} n_{0,1}^* &=& 0.019779, & n_{0,2}^* &=& 0.032472, & b_1^* &=& 3841.297958,\\ b_2^* &=& 0.000057, & \mu^* &=& 0.105982, & \sigma^* &=& 0.002643, \end{array}$$

being the error 0.006635.

In Figure 6, we show the data (points), the mean of the solution (solid curve) and confidence interval (dotted curves). The mean, $\mu_N(t)$*, has been calculated by* (24) *and* (19)–(22)*, being* $f_0(n_0, b, c) = f_{N_0}(n_0) f_B(b) f_C(c)$ *and*

$$f_{N_0}(n_0) = \begin{cases} 78.7836, & \text{if } n_0 \in [0.019779, 0.032472], \\ 0, & \text{otherwise,} \end{cases}$$

$$f_B(b) = \begin{cases} 4.119667 \cdot 10^{4203}\, \mathrm{e}^{-17542.9b}\, b^{3840.4}, & \text{if } b > 0, \\ 0, & \text{otherwise,} \end{cases}$$

$$f_C(c) = \begin{cases} 150.943\, \mathrm{e}^{-71577.4(-0.105982+c)^2}, & \text{if } 0.09 < c < 0.12, \\ 0, & \text{otherwise,} \end{cases}$$

and $t_0 = 0$*. The confidence interval has been calculated by* $\mu_N(t) \pm 1.96\sigma_N(t)$ *where* $\sigma_N(t)$ *has been calculated via* (25)*. From Figure 6 we can see that this confidence interval captures satisfactorily the uncertainty of data. In Figure 7, we show the evolution of the 1-PDF,* $f(t, n)$*, of the solution stochastic process,* $N(t)$*, together with the data (points), mean (solid curve) and confidence intervals (dotted curves). We observe that variability slightly increases as time goes on in agreement with fitting shown in Figure 6.*

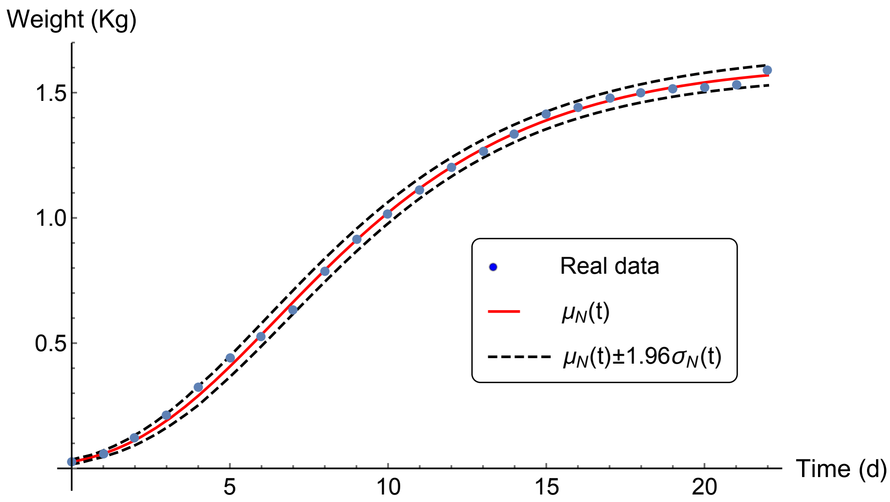

Figure 6: Model fitting: Sample data (points), expectation function (solid curve) and confidence interval (dotted curves) centred in the mean $\mu_N(t)$ and radius $1.96\,\sigma_N(t)$, being $\sigma_N(t)$ the standard deviation function. Example 2.

Now, using expression (26)*, in Figure 8 we show the PDF of random variable time* T *(in days) until the Pearl Gray Guinea Fowl species has a prefixed weight* $\rho = \rho_N$ *(in kilograms). In Table 2, we collect the expect value of* T *for different values of* $\rho = \rho_N$ *using expression* (27)*. According to these values, for example, it is expected that after* 9 *or* 10 *days, the species will weight* 1 *kg. It is worthwhile pointing out that the numerical values shown in Table 2 agree with the graphical representation shown in Figure 8.*

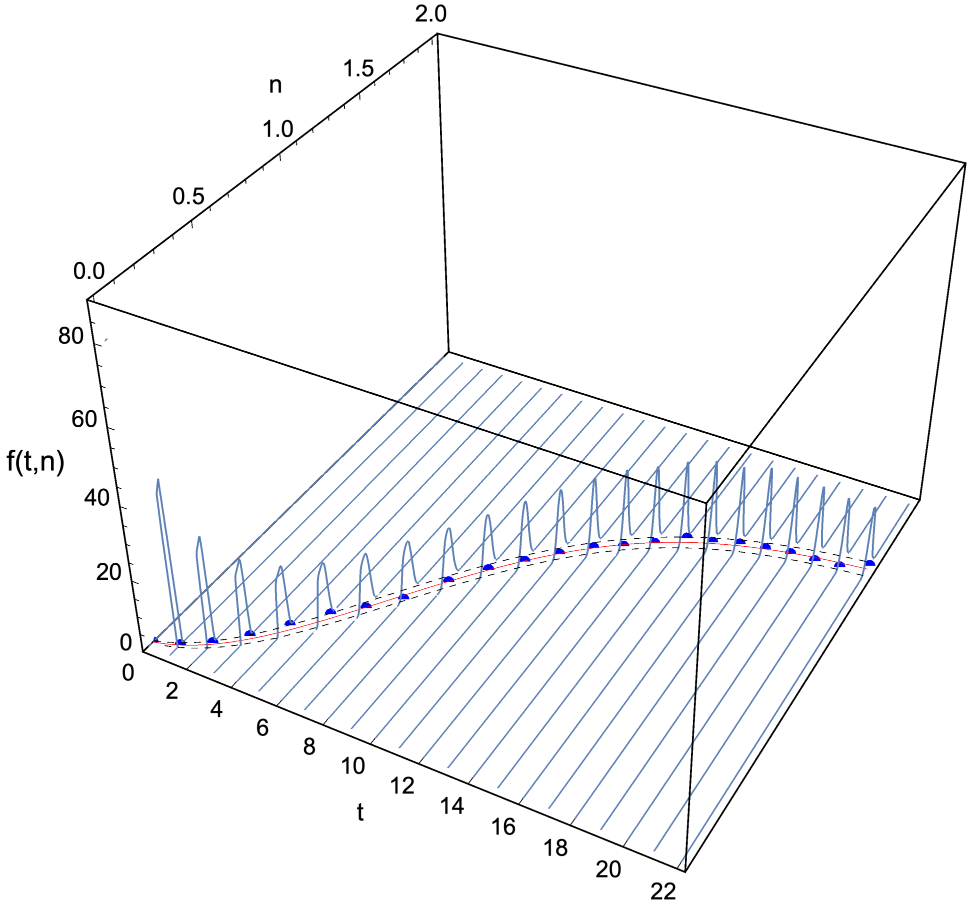

Figure 7: Representation of the 1-PDF, $f(t,n)$ of the solution stochastic process, $N(t)$, for fixed time values. In the horizontal plane $t - f(t,n)$ we have projected the plot shown in Figure 6. Example 2.

ρ_N	0.25	0.5	0.75	1	1.25	1.50
$\mu_T(\rho_N)$	3.628197	5.746689	7.682120	9.719286	12.575619	18.112325

Table 2: Expected time ($\mu_T(\rho_N)$), measured in days, needed for the weight to reach certain prefixed values (ρ_N), measured in kilograms. Example 2.

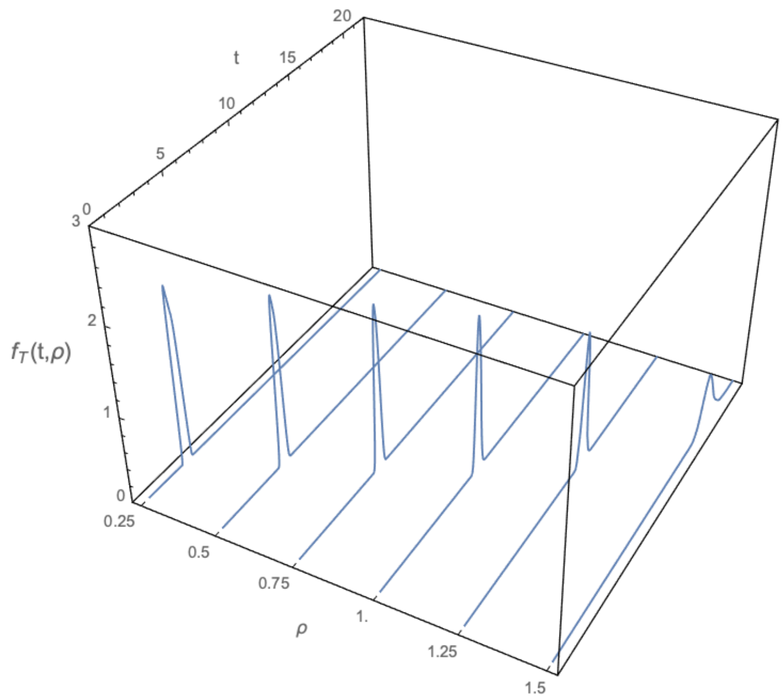

Figure 8: Graphical representation of the PDF of the random variable time T for the prefixed values of $\rho = \rho_N$ shown in Table 2. Example 2.

We conclude this example calculating, from expression (30)*, the PDF of the asymptotic state,* $N^* = \mathrm{e}^{C/B}$*,*

$$f_{N^*}(n^*) = \begin{cases} \displaystyle\int_{0.09/\ln(n^*)}^{0.12/\ln(n^*)} \frac{1}{n^*}\left(6.218349 \cdot 10^{4205} b^{2840.4}\, \mathrm{e}^{-17543.9b - 71577.4(-0.105982 + b\ln(n^*))^2}\right) \mathrm{d}b, & \text{if } n^* > 1, \\ 0, & \text{otherwise.} \end{cases}$$

Observe that, using Remark 1, the domain of integration has been determined so that $b\ln(n^*) \in (0.09, 0.12)$*, taking into account that* $B > 0$ *(recall that it has a Gamma distribution). In Figure 9, we show the PDF of the equilibrium,* $f_{N^*}(n^*)$*, as well as its mean,*

$$m^* = \int_{\mathbb{R}} n^* f_{N^*}(n^*)\, \mathrm{d}n^* = 1.622966, \tag{36}$$

and the confidence interval

$$\begin{aligned} &[m^* - 1.96\,\sigma^*, m^* + 1.96\,\sigma^*] = [1.577268, 1.668664], \\ &\sigma^* = \sqrt{\int_{\mathbb{R}} (n^*)^2 f_{N^*}(n^*)\, \mathrm{d}n^* - (m^*)^2} = 0.023315. \end{aligned} \tag{37}$$

For the sake of clarity, in Figure 10 we show a graphical representation of the model fitting together with the equilibrium including the means and confidence intervals. We can observe that for finite time (until $t = 22$*), the diameter of confidence interval increases slowly. It is expected that its maximum diameter will be reached as* $t \to \infty$*, so the confidence interval graphically represented for the equilibrium accounts this quantity. This quantifies the maximum expected uncertainty.*

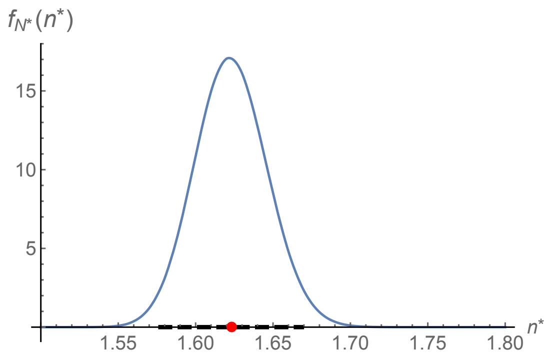

Figure 9: PDF of the equilibrium random variable $N^* = \mathrm{e}^{C/B}$. In the horizontal axis, the mean (point) and the confidence interval (dashed lines) are indicated. They have been calculated by (36) and (37), respectively. Example 2.

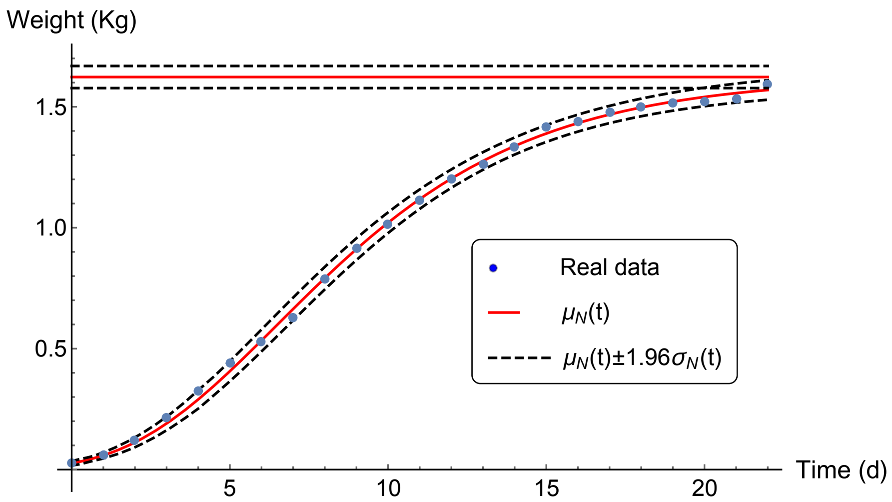

Figure 10: Graphical representation of the model fitting together with the equilibrium including the means (solid lines), confidence intervals (dotted lines) and data (points). Example 2.

5. Conclusions

In this paper we have studied, from a probabilistic standpoint, the fully randomized Gompertz model. This important model plays a key role to describe the dynamics of biological and biophysical parts of complex systems which often involve uncertainties. The study has been conducted under very general hypotheses regarding the probability distributions of model parameters, which confers a wide range of applicability to our theoretical findings. The numerical experiments and modelling carried out in the our examples show very good results. Our future efforts will concentrate on studying systems where the Gompertz model with uncertainties is a key part of the full complex model.

Acknowledgements

This work has been supported by the Spanish Ministerio de Economía, Industria y Competitividad (MINECO), the Agencia Estatal de Investigación (AEI) and Fondo Europeo de Desarrollo Regional (FEDER UE) grant MTM2017–89664–P.

Conflict of Interest Statement

The authors declare that there is no conflict of interests regarding the publication of this article.

References

References

[1] B. Blasius, J. Kurths, L. Stone, Complex Population Dynamics. Nonlinear Modeling in Ecology, Epidemiology and Genetics, Vol. 7 of Lecture Notes in Complex Systems, World Scientific, Philadelphia, 2014.

[2] L. Allen, An Introduction to Mathematical Biology, Pearson Education, New Jersey, 2007.
[3] P. Turchin, Complex Population Dynamics: A Theoretical/Empirical Synthesis, Monographs in Population Biology, Princeton University Press, New Jersey, 2003.
[4] M. Patel, J. P. Zbilut, R. E. Nagl, The Role of Model Integration in Complex Systems Modelling: An Example from Cancer Biology, Understanding Complex Systems, Springer: Complexity, Berlin Heidelberg, 2010.
[5] L. Arnold, Stochastic Differential Equations: Theory and Applications, Krieger Publishing Company, New York, 1992.
[6] B. Øksendal, Stochastic Differential Equations: An Introduction with Applications, Springer-Verlag, Berlin-Heidelberg, 2003.
[7] P. Kloeden, E. Platen, Numerical Solution of Stochastic Differential Equations, Applications of Mathematics, Springer, Berlin, 1992.
[8] D. Henderson, D. Plaschko, Stochastic Differential Equations in Science and Engineering, World Scientific, Singapore, 2006.
[9] D. Nualart, The Malliavin Calculus and Related Topics, Springer-Verlag, Berlin, 2006.
[10] G. Di Nunno, B. Oksendal, F. Proske, Malliavin Calculus for Lèvy Processes and Applications to Finance, Universitext, Springer-Verlag, Berlin, 2009.
[11] C. Braumann, Introduction to Stochastic Differential Equations with Applications to Modelling in Biology and Finance, Wiley & Sons Ltd., NJ, 2019.
[12] T. T. Soong, Random Differential Equations in Science and Engineering, Academic Press, New York, 1973.
[13] M. Loève, Probability Theory I, Vol. 45 of Graduate Texts in Mathematics, Springer-Verlag, New York, 1977.
[14] M. Loève, Probability Theory II, Vol. 46 of Graduate Texts in Mathematics, Springer-Verlag, New York, 1978.
[15] E. Wong, B. Hajek, Stochastic Processes in Engineering System, Springer Verlag, New York, 1985.
[16] D. Xiu, Numerical Methods for Stochastic Computations. A Spectral Method Approach, Princeton University Press, New Jersey, 2010.
[17] T. Neckel, F. Rupp, Random Differential Equations in Scientific Computing, Versita, London, 2013.
[18] R. C. Smith, Uncertainty Quantification. Theory, Implementation and Applications, Computational Science and Engineering, SIAM, Philadelphia, 2014.
[19] J. Golec, S. Sathananthan, Stability analysis of a stochastic logistic model, Mathematical and Computer Modelling 38 (5–6) (2003) 585–593. doi:10.1016/S0895-7177(03)90029-X.
[20] E. K. Moummou, R. Gutiérrez-Sánchez, M. Melchor, E. Ramos-Ábalos, A stochastic Gompertz model highlighting internal and external therapy function for tumour growth, Applied Mathematics and Computation 246 (2003) 1–1. doi:10.1016/j.amc.2014.08.008.
[21] J. C. Cortés, L. Jódar, L. Villafuerte, Random linear-quadratic mathematical models: Computing explicit solutions and applications, Mathematics and Computers in Simulation 79 (7) (2009) 2076–2090. doi:10.1016/j.matcom.2008.11.008.
[22] F. A. Dorini, M. S. Cecconello, M. B. Dorini, On the logistic equation subject to uncertainties in the environmental carrying capacity and initial population density, Communications in Nonlinear Science and Numerical Simulation 33 (2016) 160–173. doi:10.1016/j.cnsns.2015.09.009.
[23] F. A. Dorini, N. S. Bobko, L. B. Dorini, A note on the logistic equation subject to uncertainties in parameters, Computational and Applied Mathematics 37 (2018) 1496–1506. doi:10.1007/s40314-016-0409-6.
[24] J. C. Cortés, A. Navarro-Quiles, J. V. Romero, M. D. Roselló, Analysis of random non-autonomous logistic-type differential equations via the Karhunen–Loève expansion and the Random Variable Transformation technique, Communications in Nonlinear Science and Numerical Simulation 72 (2019) 121–138. doi:110.1016/j.cnsns.2018.12.013.
[25] J. Calatayud, J. C. Cortés, M. Jornet, Improving the approximation of the probability density function of random nonautonomous logistic-type differential equations, Mathematical Methods in the Applied Sciences 42 (2019) 7259–7267. doi:10.1002/mma.5834.
[26] M. C. Casabán, J. C. Cortés, A. Navarro-Quiles, J. V. Romero, M. D. Roselló, R. J. Villanueva, Probabilistic solution of the homogeneous Riccati differential equation: A case-study by using linearization and transformation techniques, Journal of Computational and Applied Mathematics 79 (2016) 20–35. doi:10.1016/j.cam.2014.11.028.
[27] E. Allen, Modeling with Itô Stochastic Differential Equations, Mathematical Modelling: Theory and Applications, Springer Science & Business Media B.V., Netherlands, 2007.
[28] H. Risken, The Fokker–Planck Equation Method of Solution and Applications, Springer Verlag, Berlin, 1989.
[29] S. Hesam, A. R. Nazemi, A. Haghbin, Analytical solution for the Fokker–Planck equation by differential transform method, Scientia Iranica 19 (2012) 1140–145. doi:10.1016/j.scient.2012.06.018.
[30] M. Lakestani, M. Dehghan, Numerical solution of Fokker–Planck equation using the cubic B-spline scaling functions, Numerical Methods Partial Differential Equations 25 (2009) 418–429. doi:10.1002/num.20352.
[31] X. Mao, C. Yua, G. Yin, Numerical method for stationary distribution of stochastic differential equations with Markovian switching, Journal of Computational and Applied Mathematics 174. doi:10.1016/j.cam.2004.03.016.

[32] M. C. Casabán, J. C. Cortés, A. Navarro-Quiles, J. V. Romero, M. D. Roselló, R. J. Villanueva, Computing probabilistic solutions of the Bernoulli random differential equation, Journal of Computational and Applied Mathematics 309 (2017) 396–407. doi:10.1016/j.cam.2016.02.034.

[33] B. Kegan, R. W. West, Modeling the simple epidemic with deterministic differential equations and random initial conditions, Mathematical Biosciences 195 (2005) 179–193. doi:10.1016/j.mbs.2005.02.004.

[34] J. C. Cortés, A. Navarro-Quiles, J. V. Romero, M. D. Roselló, A full solution of random autonomous first-order linear systems of difference equations. Application to construct random phase portrait for planar systems, Applied Mathematics Letters 68 (2017) 150–156. doi:10.1016/j.aml.2016.12.015.

[35] J. C. Cortés, A. Navarro-Quiles, J. V. Romero, M. D. Roselló, Solving the random Pielou logistic equation with the random variable transformation technique: Theory and applications, Mathematical Methods in the Applied Sciences 42 (2019) 5708–5717. doi:10.1002/mma.5440.

[36] F. A. Dorini, M. C. C. Cunha, On the linear advection equation subject to random velocity fields, Mathematics and Computers in Simulation 82 (2011) 679–690. doi:10.1016/j.matcom.2011.10.008.

[37] H. Slama, N. A. El-Bedwhey, A. El-Depsy, M. M. Selim, Solution of the finite Milne problem in stochastic media with RVT Technique, The European Physical Journal Plus 132. doi:10.1140/epjp/i2017-11763-6.

[38] A. Hussein, M. M. Selim, A general analytical solution for the stochastic Milne problem using Karhunen–Loeve (K–L) expansion, Journal of Quantitative Spectroscopy and Radiative Transfer 125 (2013) 84–92. doi:10.1016/j.jqsrt.2013.03.018.

[39] A. Hussein, M. M. Selim, A complete probabilistic solution for a stochastic Milne problem of radiative transfer using KLE-RVT technique, Journal of Quantitative Spectroscopy and Radiative Transfer 232 (2019) 54–65. doi:10.1016/j.jqsrt.2019.04.034.

[40] J. C. Cortés, L. Jódar, J. Camacho, L. Villafuerte, Random Airy type differential equations: Mean square exact and numerical solutions, Computers and Mathematics with Applications 60 (5) (2010) 1237–1244. doi:10.1016/j.camwa.2010.05.046.

[41] Z. Bekiryazici, M. Merdan, T. Mesemen, Modification of the random differential transformation method and its applications to compartmental models, Communications in Statistics: Theory and Methods-doi:10.1080/03610926.2020.1713372.

[42] A. K. Golmankhaneh, N. A. Porghoveh, D. Baleanu, Mean square solutions of second-order random differential equations by using homotopy analysis method, Romanian Reports in Physcis 65 (2013) 350–362.

[43] M. A. El-Tawil, The approximate solutions of some stochastic differential equations using transformations, Applied Mathematics and Computation 164 (2005) 167–178. doi:10.1016/j.amc.2004.04.062.

[44] J. Calatayud, J. C. Cortés, J. A. Díaz, M. Jornet, Constructing reliable approximations of the probability density function to the random heat PDE via a finite difference scheme, Applied Numerical Mathematics 151 (2020) 413–424. doi:110.1016/j.apnum.2020.01.012.

[45] A. T. Bharucha-Reid, Probabilistic Analysis and Related Topics, Vol. 1, Academic Press, London, 1978.

[46] M. Zak, J. P. Zbilut, R. E. Meyers, From Instability to Intelligence: Complexity and Predictability in Nonlinear Dynamics, Springer, Germany, 1997.

[47] T. L. Saaty, Modern Nonlinear Equations, Dover Publ., New York, 1981.

[48] F. Santambrogio, Optimal Transport for Applied Mathematicians. Calculus of Variations, PDEs, and Modeling, Cambridge Texts in Applied Mathematics, Birkhäuser Basel, Switzerland, 2015.

[49] G. J. Lord, C. Powell, T. Shardlow, An Introduction to Computational Stochastic PDEs, Cambridge Texts in Applied Mathematics, Cambridge University Press, UK, 2014.

[50] A. Laird, Dynamics of tumour growth: Comparison of growth rates and extrapolation of growth curve to one cell, British Journal of Cancer 19 (1965) 278–291. doi:10.1038/bjc.1965.32.

[51] S. Nahashon, S. Aggrey, N. A. Adefope, A. Amenyenu, D. Wright, Growth characteristics of Pearl Gray Guinea Fowl as predicted by the Richards, Gompertz, and Logistic Models, Poultry Science 85 (2006) 359–363.

[52] G. Casella, R. L. Berger, Statistical Inference, Cengage Learning, India, 2006.